


# *Knot Theory and the Jones Polynomial*

By:  
Wilson Poulter

Faculty Advisor:  
Dr. Maria Grazia Viola

A project submitted to the Department of Mathematical Sciences in conformity with the  
requirements for Math 4301 (Honours Seminar)

Lakehead University  
Thunder Bay, Ontario, Canada

Attribution-ShareAlike 4.0 International  2018 Wilson Poulter

## **Abstract**

In this paper we introduce the notion of a knot, knot equivalence, and their related terms. In turn, we establish that these terms correspond to the much simpler knot diagram, Reidemeister moves, and their related terms. It is then shown that working with these latter terms, one can construct a number of invariants that can be used to distinguish inequivalent knots. Lastly, the use of these invariants is applied in setting of molecular biology to study DNA supercoiling and recombination.

# Contents

<b>1</b>	<b>Introduction</b>	<b>1</b>
<b>2</b>	<b>Preliminaries</b>	<b>2</b>
2.1	Knots and Knot Equivalence . . . . .	2
2.2	Polygonal Knots . . . . .	3
2.3	Orientation and Links . . . . .	4
<b>3</b>	<b>Knot Diagrams and Reidemeister Moves</b>	<b>6</b>
3.1	Knot Diagrams . . . . .	6
3.2	Reidemeister Moves . . . . .	8
<b>4</b>	<b>Link invariants</b>	<b>16</b>
4.1	Linking Number . . . . .	16
4.2	The Alexander–Conway Polynomial . . . . .	18
<b>5</b>	<b>The Jones Polynomial</b>	<b>22</b>
5.1	The Kauffman Bracket . . . . .	22
5.2	The Normalized Kauffman Bracket . . . . .	25
5.3	The Jones Polynomial . . . . .	27
<b>6</b>	<b>Applications to Molecular Biology</b>	<b>30</b>
6.1	Supercoiling . . . . .	30
6.2	Recombination . . . . .	31

# 1 Introduction

Although this paper discusses knots from a formal mathematical perspective, knots, until recently, have been of only technical and cultural concern. In 1700 BCE, before written language, it is believed that a Mesopotamian merchant used engravings of knots on his coins to indicate their value. The Greek physician Heraklas wrote instructions on how to knot orthopedic slings sometime in the first century [7]. Knots can also be found ornamenting objects associated with Buddhism, Christianity, and Hinduism. Moreover, in coastal economies, nets for fishing were constructed by the skilled knotting of ropes.

Perhaps the mathematical idea of a knot can be derived from Leibniz's comments on the need for a 'geometry of positions' over a 'geometry of magnitudes' [7]. The comment's relevance is this: we tend not to think of knots as having a precise structure; two knotted strings can look different, yet both be the same knot. For example, the instructions children use for tying their shoes do not reference precisely how much of the lace should be used at certain steps, nor the angles at which the laces should be positioned. Indeed, these instructions only refer to bunny ears and rabbit holes. Given this imprecision, it is hard to imagine that a child's shoe is ever tied twice in the same manner. Nonetheless, these instructions always produce the same knot.

To motivate our mathematical study of knots then, we wish to develop a theory of knots that maintains some level of this notion of position in place of magnitude. Imprecisely, we will say that two knots are the same if one can be wiggled around and stretched so that it looks like the other one, without ever cutting and pasting it [8]. Note however that under this definition, every knot from our everyday life is the same knot! To elaborate, whenever we tie a knot, there's always a procedure to untie it, so all of these 'knots' are the same as a string with no knots in it. Thus, we add a feature peculiar to our everyday experience of knots, which is to glue these two loose strands together once the knot is tied, as this prevents us from untying the knot as before [2]. Once this procedure has been completed, if we can still wiggle and stretch one knot to look like another without ever cutting and pasting it, then these two knots are the same.

But, what if two knots are different? How can we demonstrate this? Indeed, there are many different ways to wiggle around the strings of a knot, so many in fact, that failing to wiggle one knot into another for the entirety of your life would not conclusively show that those two knots are different. In the pages that follow, we will introduce the ideas of knot theory formally, and address how we might demonstrate the difference of two knots. In particular, we will show that there are indeed 'knotted' knots and that moreover, some knots are different from their 'mirror image,' which we will demonstrate by eventually distinguishing all the knots in Figure 1.

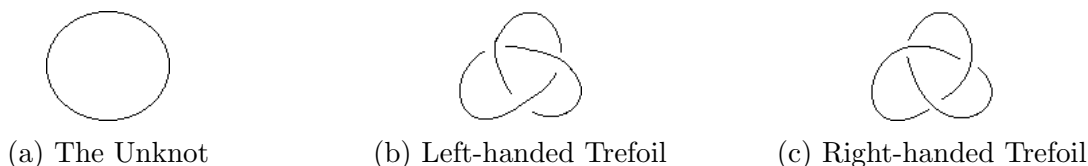


Figure 1: Different Types of Knots

## 2 Preliminaries

To begin our investigation, we introduce the formal definition of our object of interest, the knot.

### 2.1 Knots and Knot Equivalence

**Definition 2.1.** A knot  $K$  is an embedding  $K : \mathbb{S}^1 \hookrightarrow \mathbb{R}^3$

Note that by our definition, knots can be thought of simply as non-intersecting loops in three dimensions.

**Definition 2.2.** A knot  $K_1$  is equivalent to another knot  $K_2$  if there exists a continuous function  $H : \mathbb{R}^3 \times [0, 1] \rightarrow \mathbb{R}^3$ , such that  $H_t(x)$  is a homeomorphism for all fixed  $t \in [0, 1]$ ,  $H_0(x) = id_{\mathbb{R}^3}$  and  $H_1 \circ K_1 = K_2$ .  $H$  is said to take  $K_1$  to  $K_2$ .

This definition justifies our insistence that knots be looped, as all knots that are strictly a paths would be equivalent, trivializing many knots.

Before continuing our discussion, we verify that knot equivalence is indeed an equivalence relation on the class of knots.

**Proposition 2.3.** Knot equivalence is an equivalence relation.

*Proof.* Consider first a knot  $K_1$ . We define  $H : \mathbb{R}^3 \times [0, 1] \rightarrow \mathbb{R}^3$  by  $H_t(x) = x$ , then  $H$  takes  $K_1$  to itself, so knot equivalence is a reflexive relation.

Suppose now that  $K_1$  is equivalent to  $K_2$ , and  $H$  as in Definition 2.2. Since  $H_t(x)$  is an homeomorphism for every  $t \in [0, 1]$ , it has an inverse  $H_t^{-1}(x)$  that is also a homeomorphism for every  $t \in [0, 1]$ . We see then that  $G : \mathbb{R}^3 \times [0, 1] \rightarrow \mathbb{R}^3$  where  $G_t(x) = H_t^{-1}(x)$  for each  $t$ , is itself continuous. Since  $H_0(x) = id_{\mathbb{R}^3}$ ,  $G_0(x) = id_{\mathbb{R}^3}$ . Also, since  $H_1 \circ K_1 = K_2$ ,  $K_1 = G_1 \circ K_2$ , and thus  $K_2$  is equivalent to  $K_1$ .

Lastly, if  $H : \mathbb{R}^3 \times [0, 1] \rightarrow \mathbb{R}^3$  takes  $K_1$  to  $K_2$ , and  $G : \mathbb{R}^3 \times [0, 1] \rightarrow \mathbb{R}^3$  takes  $K_2$  to  $K_3$ , where each  $K_i$  is a knot, define  $F_t = G_t \circ H_t$  for all  $t \in [0, 1]$ . Clearly  $F : \mathbb{R}^3 \times [0, 1] \rightarrow \mathbb{R}^3$  is continuous, and  $F_t$  is a homeomorphism for all  $t$ . Also

$$\begin{aligned} F_0 &= G_0 \circ H_0 = id_{\mathbb{R}^3} \circ id_{\mathbb{R}^3} = id_{\mathbb{R}^3} \\ F_1 \circ K_1 &= G_1 \circ H_1 \circ K_1 = G_1 \circ K_2 = K_3 \end{aligned}$$

So  $F$  takes  $K_1$  to  $K_3$ , and knot equivalence is thus a transitive relation.  $\square$

While these definitions may seem to satisfy our idea of what a knot is, and when two knots should be considered the same, it is perhaps not restrictive enough. Indeed, this definition allows for the case of ‘pathological’ or ‘wild’ knots. For example, a knot by our definition could have an infinite number of smaller knots within it, as in Figure 2.

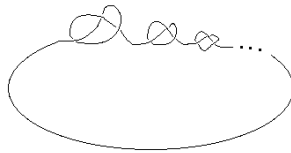


Figure 2: An example of a ‘wild knot’

To exclude these types of cases, we introduce a simpler definition of a knot.

## 2.2 Polygonal Knots

**Definition 2.4.** A polygonal knot  $K$  is a non-intersecting polygon in  $\mathbb{R}^3$ .

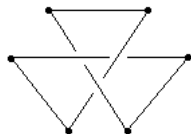


Figure 3: A polygonal knot

Since polygons have only a finite number of edges and vertices, we can see that a knot according to this definition will not exhibit the ‘pathological’ properties of the wild knot discussed above. Moreover, this allows us to have a very simple definition of knot equivalence that conforms to our more general notion of a knot given above. That is, a knot in this new sense is also the image of a knot in the former sense.

**Definition 2.5.** A polygonal knot  $K_1$  is equivalent to another polygonal knot  $K_2$  if one can apply the following operations to  $K_1$  (and its intermediate knots) a finite number of times, and obtain  $K_2$ .

- (i) Suppose  $AB$  is an edge in a knot  $K$ ,  $C$  is a point other than  $A$  or  $B$ , and that the interior of the triangle  $ABC$  contains no points of  $K$ . Then the edge  $AB$  may be deleted and replaced with the edges  $AC$  and  $BC$ .
- (ii) Suppose  $AC$  and  $BC$  are edges in a knot  $K$ . If the only points of  $K$  contained in the closed triangle  $ABC$  are those in  $AC$  and  $BC$ , then the edges  $AC$ , and  $BC$ , as well as the point  $C$  may be deleted, and replaced with the edge  $AB$ .

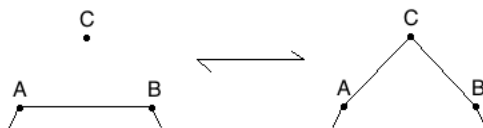


Figure 4: A valid  $\Delta$ -move on a plane in  $\mathbb{R}^3$

**Remark 2.6.** The second operation can be thought of as the inverse of the first operation. Indeed, given the application of the first operation, the conditions are met for one to subsequently apply the second operation (where the points  $A$ ,  $B$ , and  $C$  considered are the same as they were in the first operation). Doing so, one obtains the original knot. This concept of invertibility is of course applicable as well when the second operation is applied first. We refer more generally to these operations as ‘ $\Delta$ -moves’.

**Remark 2.7.** A valid  $\Delta$ -move can be defined without ambiguity by the triangle  $ABC$ . Indeed, if a  $\Delta$ -move is valid, either (i)  $A$  and  $B$  are vertices of  $L$  but  $C$  is not, or (ii) all  $A$ ,  $B$ , and  $C$  are vertices of  $L$ . These two cases correspond respectively to the operation defined above.

Like before, we should also show that our definition here truly defines an equivalence relation.

**Proposition 2.8.** Knots that are related by  $\Delta$ -moves form an equivalence class on knots.

*Proof.* First, if  $K_1$  is a knot, then applying the empty sequence of  $\Delta$ -moves on  $K_1$  results in the knot  $K_1$ , so  $K_1$  is equivalent to  $K_1$ .

Secondly, suppose there exists a sequence of  $\Delta$ -moves on  $K_1$  that produces  $K_2$ . If one replaces all of the  $\Delta$ -moves in the sequence with their inverse (see Remark 2.6.) and then reverses the order of the operators in the sequence, we see that this ‘reversed’ sequence produces  $K_1$  from  $K_2$ .

Lastly, if there are two finite sequences of  $\Delta$ -moves which produce  $K_2$  from  $K_1$ , and  $K_3$  from  $K_2$  respectively, then modifying the index on the sequence from  $K_2$  to  $K_3$  so that its  $i^{th}$  operation is now labelled  $n + i$ , where  $n$  is the length of the sequence from  $K_1$  to  $K_2$ , and concatenating the sequences from  $K_1$  to  $K_2$  and  $K_2$  to  $K_3$ , we obtain a sequence that produces  $K_3$  from  $K_1$ .  $\square$

As one may have suspected,  $\Delta$ -moves are themselves an example of an  $H$  from Definition 2.2. So, when two polygonal knots are said to be equivalent under  $\Delta$ -moves, we are more generally speaking of two knots being equivalent. Additionally, it can be shown that the class of polygonal knots is equivalent to a very large, and well behaved, class of non-polygonal knots. Thus, polygonal knots serve as a very suitable definition of a knot. Sketches of the proof of these facts is found in Section 1.11. of [2].

Before proceeding to the next section, we introduce two notions that follow easily from the above discussion

## 2.3 Orientation and Links

It will be useful at times to consider knots with an orientation. The orientation can be thought of as a choice of direction to travel along the knot. To indicate a knot's orientation, we include arrows on its diagram (more on knot diagrams in the next section). Thus, we can assign every knot two orientations, as seen in Figure 5 below.

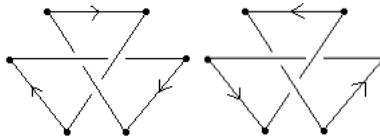


Figure 5: Two orientations of the same knot

For oriented knot equivalence, we use instead of just a standard knot equivalence  $H$ , an orientation preserving knot equivalence  $H$ .

In the case of polygonal knots, an ‘oriented  $\Delta$ -move’ is just the usual  $\Delta$ -move, with the caveat that the resultant knot retains the orientation of the original. Then two oriented polygonal knots are equivalent if one can be transformed into the other by a sequence of oriented  $\Delta$ -moves.

**Definition 2.9.** A *link* is an injective mapping  $L : \prod_{k=1}^n \mathbb{S}_k^1 \rightarrow \mathbb{R}^3$  where  $\mathbb{S}_k^1 = \mathbb{S}^1$ , and  $L|_{\mathbb{S}_k^1}$  is a knot for all  $k \in \{1, \dots, n\}$ .

In accordance with our earlier simplification however, we again modify this definition so that a link is defined in terms of polygons.

**Definition 2.10.** A polygonal link is a finite union of polygonal knots, such that the intersection of any two knots in the union is empty.



Figure 6: A Hopf link

In light of this, we can see that two polygonal links will be equivalent if there exists a sequence of  $\Delta$ -moves that transforms one into the other. Note that a knot is also by definition a link.

Links may also have orientations, like knots. Following from the idea of an oriented knot, we just assign each component of the link an orientation. Thus, if a link has  $n$  components, it has  $2^n$  potential orientations.



### 3 Knot Diagrams and Reidemeister Moves

In the last section, we adopted the convention that knots and links are unions of closed polygons for two reasons. The first was to eliminate pathological cases of knots. The second reason, which we will elaborate more on in this section, is because it allows us to approach knot theory using a knot's combinatoric properties. In light of this, throughout the rest of the paper we shall refer to polygonal knots and links simply as knots and links respectively.

Let us introduce another definition that will allow us to simplify our concept of knots even further.

#### 3.1 Knot Diagrams

**Definition 3.1.** (Definition 2.2.1 of [8]) A *link diagram*  $D$  is the image of a link  $L$  under the projection  $\pi : \mathbb{R}^3 \rightarrow \mathbb{R}^2$  with  $\pi(x, y, z) = (x, y)$  such that

- (i) For all  $(x, y) \in \mathbb{R}^2$ ,  $|\pi^{-1}(x, y) \cap L| \leq 2$ .
- (ii) If  $V$  is a vertex of  $L$ , and  $\pi(V) = (x, y)$  then  $|\pi^{-1}(x, y) \cap L| = 1$ .
- (iii) Only finitely many  $(x, y) \in \mathbb{R}^2$  satisfy  $|\pi^{-1}(x, y) \cap L| = 2$

Additionally, when  $\pi^{-1}(x, y) \cap L = \{(x, y, z_1), (x, y, z_2)\}$ , with  $z_1 < z_2$ , there is a marking (elaborated below) indicating which edge of  $L$  the point  $(x, y, z_1)$  belongs to.

Less formally, the three conditions above are provided so that our diagrams contain as much information as possible about the knot in question. In the first condition, we are insisting that at most two edges intersect at a single point in the projection. This simplifies the process for distinguishing the vertical relationship between edges in the actual link. In the second one we want to be able to see exactly where the vertices are in our diagram, and to which edges they belong. For the third condition, we insist that no edge projects directly atop another one. Also, for the last caveat, it is customary in a link diagram to erase the lower edge in a small neighbourhood of the point in question. The point in question is referred to as a crossing point, and the lower edge is said to cross under the upper edge. By condition (iii), we see that there will only be a finite number of crossing points in any link diagram.

We would also like to show that, since a link diagram  $D$  can represent many links (uncountably many in fact), that all these links are in fact equivalent to one another.

**Proposition 3.2.** If  $L_1$  and  $L_2$  have the same link diagram  $D$ , then  $L_1$  is equivalent to  $L_2$ .

*Proof.* We transform  $L_1$  and  $L_2$  by a sequence of  $\Delta$ -moves so that their final resultants are equal.

First, note that we can assume that  $v$  is a vertex of  $L_1$  if and only if there is a vertex  $v'$  of  $L_2$  with  $\pi(v) = \pi(v')$ . This is the case because for any vertex  $v$  in the diagram of  $L_1$ , if  $\pi^{-1}(v) \cap L_2$  corresponds to a point on  $L_2$  that is not a vertex, we apply the  $\Delta$ -move to  $L_2$  on a triangle with empty interior (called the trivial  $\Delta$ -move) to obtain a new vertex  $v'$ , with  $\pi(v) = \pi(v')$ . Repeating the process but the roles of  $L_1$  and  $L_2$  reversed, we obtain diagrams with this property.

Now, without loss of generality, assume the  $z$ -coordinate of a vertex  $v_0$  of  $L_1$  is less than the  $z$ -coordinate of the vertex  $v'_0$  in  $L_2$ , with  $\pi(v_0) = \pi(v'_0)$  (henceforth,  $v_i$  denotes a vertex in  $L_1$  and  $v'_i$  denotes a vertex in  $L_2$ , with  $\pi(v_i) = \pi(v'_i)$ ). In what follows, we will show that via  $\Delta$ -moves  $L_1$  can be transformed into a link with  $v'_0$  as a vertex, and without  $v_0$ .

Consider a vertex  $v_1$ , adjacent to  $v_0$  in  $L_1$ . If the  $z$ -coordinate of  $v_1$  is less than the  $z$ -coordinate of  $v'_1$  as well, then  $v_0v_1$  lies below  $v'_0v'_1$ . Otherwise they intersect at some point,  $v^*$ . If this is the case, then add  $v^*$  to both links by the trivial  $\Delta$ -move, and have it replace both  $v_1$  and  $v'_1$  respectively in the rest of the proof.

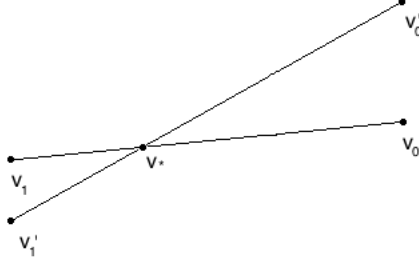


Figure 7:  $v^*$

Now, if the intersection of the interior of the triangle formed by  $v_0$ ,  $v'_0$  and  $v_1$  and  $L_1$  is empty, then we can construct a  $\Delta$ -move on these points that adds  $v'_0$  to  $L_1$ .

If not, then there is at least one segment  $S$  of  $L_1$  that crosses over  $v_0v_1$  (but below  $v'_0v'_1$ ) and through the interior of the triangle formed by  $v_0$ ,  $v'_0$  and  $v_1$ . Since  $L_2$  has the same link diagram as  $L_1$ , there is a segment  $S'$  of  $L_2$  that crosses over  $v'_0v'_1$ , and  $\pi(S) = \pi(S')$ .

Due to the properties of a link diagram, there is a sufficiently small section of  $S$  with only one crossing point (where  $S$  crosses over  $v_0v_1$ ). Thus, this section may be freely lifted above  $v'_0v'_1$  through  $\Delta$ -moves. Explicitly, this is accomplished by adding trivial vertices  $v_3$  and  $v_4$  on the boundary points of the above mentioned section of  $S$ , as well as  $v'_3$  and  $v'_4$  to  $S'$ . Then, taking some point  $v'_5$  on  $S'$  between  $v'_3$  and  $v'_4$  that does not project onto  $v_0v_1$  and make a  $\Delta$ -move on  $L_1$  with the triangle formed by  $v_3$ ,  $v'_5$ , and  $v_4$ , as well as adding trivially  $v'_5$  to  $L_2$ . Now, choose some point  $v'_6$  on  $S'$  similarly as we did for  $v'_5$ , but ensure that it lies on the opposite side of  $v_0v_1$  in comparison to  $v'_5$ . Then construct a  $\Delta$ -move on  $L_1$  with  $v'_5$ ,  $v'_6$ , and  $v_4$ , and also trivially add  $v'_6$  to  $S'$ . We thus create a quadrilateral region that lifts this section of  $S$  above  $v'_0v'_1$  (see Figure 8).

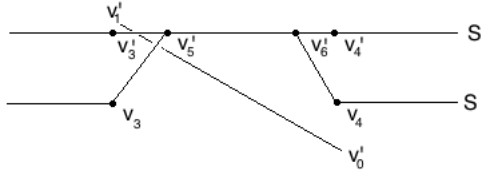


Figure 8: The quadrilateral region from the section in  $S$  via  $\Delta$ -moves

Completing this process with all the crossing points between  $v_0$  and  $v_1$  ensures that the intersection of the interior of the triangle formed by  $v_0$ ,  $v'_0$  and  $v_1$  and  $L_1$  is empty, so  $v'_0$  may be added to  $L_1$  by a  $\Delta$ -move.

Since we have added  $v'_0$  to  $L_1$ , we need to delete  $v_0$  from  $L_1$ . To do this, take the vertex  $v_3$  adjacent to  $v_0$  that is distinct from  $v'_0$ . Complete the above process again, so that the intersection of the interior of the triangle formed by  $v_0$ ,  $v'_0$  and  $v_3$  and  $L_1$  is empty, *but*, change the  $\Delta$ -move on  $v_0$ ,  $v'_0$  and  $v_3$  to be the inverse type that deletes  $v_0$ .

Note that throughout this process, all of our transformations eventually resolved into a knot with a valid diagram. We also maintained a one-to-one correspondence between the vertices of our transformations, even when adding and deleting vertices. Moreover, we only need to add vertices when there exist segments  $S$  of  $L_1$ . Since we do not add any new crossing points to the diagram of the transformed  $L_1$  throughout this process, after sufficiently many vertices have been added to construct the  $\Delta$ -moves in Figure 8, there is no longer a need to add any more vertices to  $L_1$  and  $L_2$ , so eventually it will be the case that  $L_1$  is transformed by  $\Delta$ -moves into  $L_2$ .  $\square$

The reader may realize that under this definition, not all links have diagrams. For example, the triangle with corners at  $(0,0,0)$ ,  $(0,1,0)$ , and  $(0,0,1)$  in  $\mathbb{R}^3$  will have the clearly invalid projection  $\{(0,t) : 0 \leq t \leq 1\}$  in  $\mathbb{R}^2$ . However, the definition and remark that follow show that a link can always be associated to an appropriate link diagram.

**Definition 3.3.** (Definition 2.2.3 in [8]) An  $\epsilon$ -perturbation of a link  $L$  is a displacement of the vertices of  $L$  by a euclidian distance less than  $\epsilon$ , such that connecting the vertices by edges in the same manner as  $L$  is also a link.

**Remark 3.4.** (Fact 2.2.4 in [8]) For any link  $L$ , there exists an arbitrarily small  $\epsilon$ -perturbation of  $L$  that is equivalent to  $L$ , and has a link diagram.

Thus, if  $L$  does not have a diagram, we can still associate it with a link diagram. Since we are studying the properties of links from a topological point of view, their exact projection is not so important; what is important is the relationship between the edges. In the rest of the section, we will show that knowing a links diagram, and some simple operations on them, is enough to determine whether or not two links are equivalent.

## 3.2 Reidemeister Moves

**Definition 3.5.** A *planar isotopy* ( $R_0$ ) of a link diagram is just the image of a  $\Delta$ -move on the diagram's corresponding link, such that the projection of the interior of the triangle in which it takes place in does not intersect any of the link diagram.

**Definition 3.6.** (Figure 2 of [1]) Given a link diagram  $D$ , we can form a new diagram  $D'$  by applying to  $D$  one of the moves shown below (up to planar isotopy). These operations are termed *Reidemeister Moves of Type I, II, and III*. If two diagrams are related by a sequence of Reidemeister moves, we say that they are *ambient isotopic*.

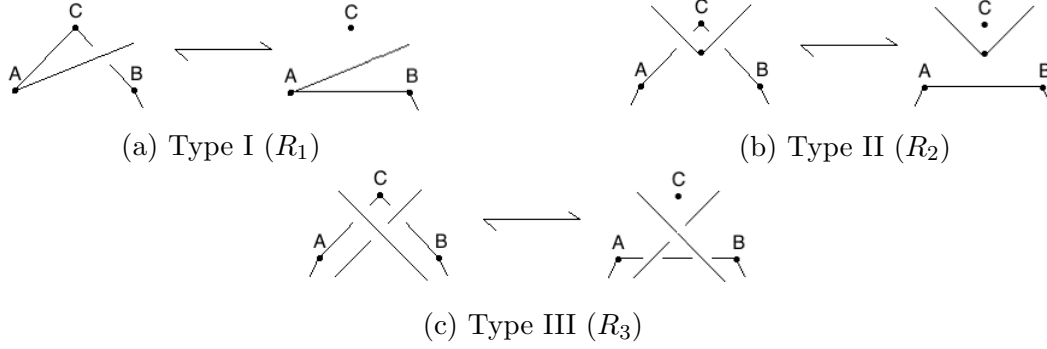


Figure 9: The three Reidemeister moves

As we will show in the next theorem, the link diagram that results from applying one of the Reidemeister moves to the diagram  $D$  is in fact a diagram of a link associated to  $D$ .

**Proposition 3.7.** Two links,  $L_1$  and  $L_2$  are equivalent if their link diagrams are ambient isotopic.

*Proof.* In the case of the Reidemeister move of type I, it suffices to show that the segment having a vertex at  $A$  and crossing over  $BC$  *cannot* be in the interior of the triangle  $ABC$  in  $\mathbb{R}^3$ , so that the interior of  $ABC$  is empty with respect to  $L$ , and the  $\Delta$ -move in  $ABC$  is valid. To show this, we note that if a line intersects a plane more than once, it intersects a plane everywhere. Now, the segment in question clearly intersects the plane described by  $A$ ,  $B$ , and  $C$  at least once, since its vertex is  $A$ . However, the segment crosses over  $BC$ , so it follows that some of the segment does not intersect the plane. Thus, the segment intersects the plane only at  $A$ , which is outside the interior of the triangle formed by  $A$ ,  $B$ , and  $C$ .

For the Reidemeister moves of type II and III, it may not be the case that the equivalence can be found with only one  $\Delta$ -move for an arbitrary knot. However, by Proposition 3.2. all we must show is that for any two links with diagrams related by either of these two Reidemeister moves, there are links with the given diagrams that are equivalent. To illustrate this idea for arbitrary link diagrams, examine Figure 10 below. Suppose a link diagram has a compact neighbourhood that is planar isotopic to Figure 9b or 9c. Moreover, the link diagram can be covered by a compact neighbourhood. Define  $R$  to be the intersection of the link diagram with the difference of these two neighbourhoods. We then take  $\pi^{-1}(R)$  as given, so that in particular the  $z$ -coordinates of the parts link on the boundary of  $R$  are given. Within this neighbourhood however, we choose the  $z$ -coordinates so that there is a  $\Delta$ -move that gives the diagram following a Reidemeister move. For notational simplicity below, if  $v$  is a labelled point on the diagram, then  $(v, z_0)$  refers to the point in  $\mathbb{R}^3$  with  $\pi(v, z_0) = v$ , and  $z$ -coordinate of  $z_0$ .

For the type II move, refer to Figure 10. Let  $z_0$  equal the least  $z$ -coordinate between  $\pi^{-1}(v_1)$  and  $\pi^{-1}(v_2)$ . Define the coordinates of the vertices of  $L$  to be  $(A, z_0), (B, z_0), (C, z_0), (v_3, z_0 + 1)$ . Clearly, there is a  $\Delta$ -move on the triangle  $(A, z_0), (C, z_0), (B, z_0)$ .

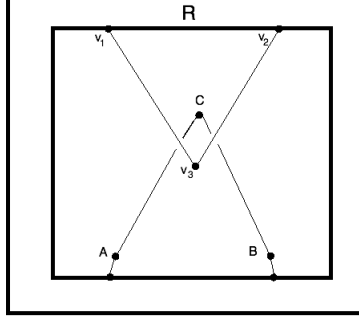


Figure 10: Diagram of an arbitrary  $R_2$  move

For the type III move, refer to Figure 11. Pick some  $z_0 \in \mathbb{R}$ . Then let the vertices of  $L$  in  $\mathbb{R}^3$  be  $(A, z_0), (B, z_0), (C, z_0), (v_3, z_0 + 2), (v_4, z_0 + 1), (v_5, z_0 + 1), (v_6, z_0 + 2)$ . Clearly then, there is a  $\Delta$ -move on the triangle  $(A, z_0), (C, z_0), (B, z_0)$ .  $\square$

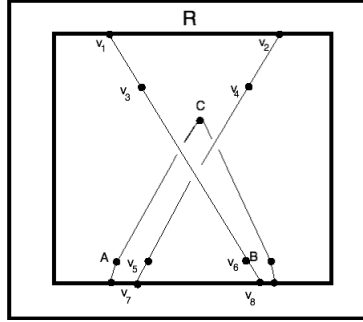


Figure 11: Diagram of an arbitrary  $R_3$  move

Thus, diagrams related by a sequence of Reidemeister moves represent the same knot. To finish this section, we give a sketch of the proof of the converse of this proposition. This theorem is a powerful tool for proving link invariants.

**Theorem 3.8.** ( See [1]) Two links  $L_1$  and  $L_2$  are equivalent if and only if their link diagrams  $D_1$  and  $D_2$  are ambient isotopic.

*Sketch of Proof.* One direction is given by the proof of Proposition 3.7. Note for the proof of the other direction, it is sufficient to show that two knot diagrams different by single  $\Delta$ -deformation are related by a sequence of Reidemeister moves. For the purposes of this proof, we introduce the notion of a  $\Delta$ -factorization. Given some  $\Delta$ -move on a link  $L$  (call it  $\Delta$ ), a  $\Delta$ -factorization of  $\Delta$  is a sequence of  $\Delta$ -moves  $(\Delta_i)_{i=1}^n$  on  $L$ , such that the triangles of  $\Delta_i$  are contained in the triangle of  $\Delta$ , and the link obtained from  $L$  by applying the sequence of  $\Delta$ -moves to  $L$  is the same as the link obtained by applying  $\Delta$  to  $L$ .

Now, consider the diagrams of two links related by a  $\Delta$ -move. There may also be other parts of the diagram interior to the triangle in the projection. If not, the two diagrams are related by a planar isotopy.

Thus, assume that the interior of the triangle in the projection is not empty. We wish to consider three specific objects that may be present: crossing points in the interior of the

triangle, vertices in the interior of the triangle, and edges that have neither crossing points nor vertices in the interior of the triangle. Denote the set of these objects by  $C(\Delta), V(\Delta), E(\Delta)$ . By the nature of a link diagram, these sets are all finite. We proceed based on the cardinality of these sets.

(i) If for a  $\Delta$ -move,  $|C(\Delta)| + |V(\Delta)| > 1$ , then we find a  $\Delta$ -factorization  $(\Delta_i)_{i=1}^2$  such that for any  $i$ ,  $|C(\Delta_i)| + |V(\Delta_i)| < |C(\Delta)| + |V(\Delta)|$ . To do so, pick two crossing points, vertices, or one of each. Call them  $e_1$  and  $e_2$ . Then, there is some vertex  $v_1$  of  $\Delta$  that is not collinear with  $e_1$  and  $e_2$ . Now, consider the line segment between  $e_1$  and  $e_2$ ,  $S$ . We construct  $\Delta_1$  by picking a point  $p$  on the side of  $\Delta$  opposite  $v_1$ , such that the segment  $S'$  between  $p$  and  $v_1$  intersects  $S$ , and  $S'$  does not contain any crossing points or vertices in the interior of  $\Delta$ . Choosing a vertex  $v_2$  in  $\Delta$  distinct from  $v_1$ , let the triangle formed between  $v_2$ ,  $p$ , and  $v_1$  be  $\Delta_1$ , and  $\Delta_2$  be the triangle formed by  $p$ ,  $v_1$ , and the remaining vertex  $v_3$  of  $\Delta$ . Refer to Figure 12 below.

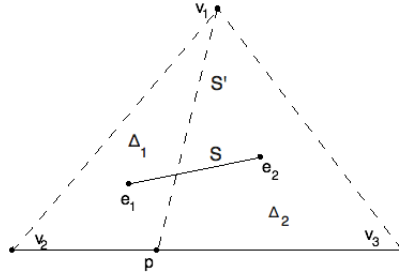


Figure 12: A  $\Delta$ -factorization for (i)

(ii) If for a  $\Delta$ -move,  $|C(\Delta)| + |V(\Delta)| = 1$ , and  $|E(\Delta)| > 0$ , we find a factorization  $(\Delta_i)_{i=1}^3$  with  $|C(\Delta_i)| + |V(\Delta_i)| = 0$  if  $i \neq 1$  and  $|E(\Delta_1)| < |E(\Delta)|$ . Choose an edge  $E$  in  $E(\Delta)$ , and call the crossing point/vertex  $p$ . Due to the properties of link diagrams, we know  $p$  is not on  $E$  in the diagram, and moreover  $E$  divides  $\Delta$  into two different polygonal regions. Further,  $p$  lies in the interior of one of these regions, call it  $\Omega$ . Choose a vertex  $v_1$  of  $\Delta$  such that  $v_1$  is also a vertex of  $\Omega$ , and  $v_1$  is not on  $E$ . Now, taking a vertex  $v_2$  of  $\Delta$  that is not in  $\Omega$ , choose points  $e$  on  $E$  and  $e'$  on the boundary of  $\Delta$ , such that  $v_2$ ,  $e$ , and  $e'$  are collinear, and the triangle formed by  $v_1$ ,  $e$ , and  $e'$  contains  $p$ . Denote this triangle by  $\Delta_1$ . Let  $\Delta_2$  be formed by  $v_1$ ,  $v_2$ , and  $e$ , while  $\Delta_3$  be formed by  $v_2$ ,  $e'$ , and  $v_3$ , where  $v_3$  is the remaining vertex of  $\Delta$ . Refer to Figure 13 below.

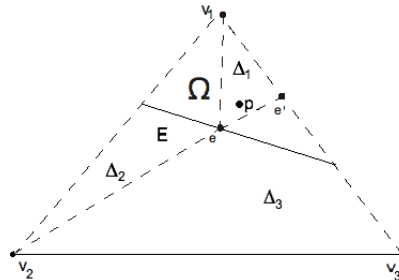


Figure 13: A  $\Delta$ -factorization for (ii)

(iii) If  $|C(\Delta)| = 0$ ,  $|V(\Delta)| = 0$ , and  $|E(\Delta)| > 1$ , choose a factorization  $(\Delta_i)_{i=1}^3$  such that  $|E(\Delta_1)|, |E(\Delta_2)|, |E(\Delta_3)| < |E(\Delta)|$ . Choose two edges, call them  $E_1$  and  $E_2$ .  $E_1$  and  $E_2$  bound a non-empty polygonal region  $\Omega$  in  $\Delta$ . Within  $\Omega$ , there exists a segment  $S$  such that  $S$  does not intersect  $E_1$  nor  $E_2$  in the interior of  $\Delta$ . Label the points where  $S$  intersect the boundary of  $\Delta$  by  $e$  and  $e'$ . Then  $e, e'$  and a vertex  $v_1$  of  $\Delta$  form a triangle that contains neither  $E_1$  or  $E_2$ . Let this be  $\Delta_1$ . Let  $\Delta_2$  be formed by  $e, e'$  and  $v_2$  where  $v_2$  is a vertex of  $\Delta$  distinct from  $v_1$ , and  $\Delta_3$  by  $e', v_1$ , and  $v_3$ , where  $v_3$  is the remaining vertex of  $\Delta$ . Refer to Figure 14 below.

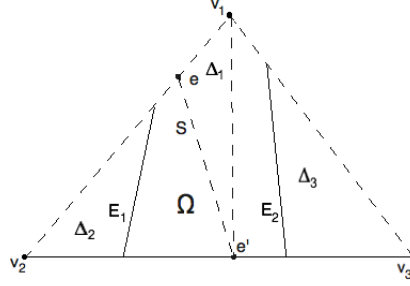


Figure 14: A  $\Delta$ -factorization for (iii)

By factoring all  $\Delta$ -moves by rule (i), then once all valid cases are exhausted using rule (ii), etc., we obtain factors that each have only a single crossing point, vertex, or edge. We must show that these diagrams of these factors are equivalent under Reidemeister moves. We only examine the case in which there is one edge in the diagram of the  $\Delta$ -move, since the proof is long and tedious.

Denote by  $A, B$ , and  $C$  the vertices of  $\Delta$ . Suppose that the vertex of the edge is in  $\Delta$ , then the vertex is either  $A$  or  $B$ . If the vertex is  $B$ , then we can find a factorization  $(\Delta_i)_{i=1}^2$  in which  $B$  becomes like  $A$ . Such a factorization is given by any edge drawn from  $C$ , as shown in Figure 15.

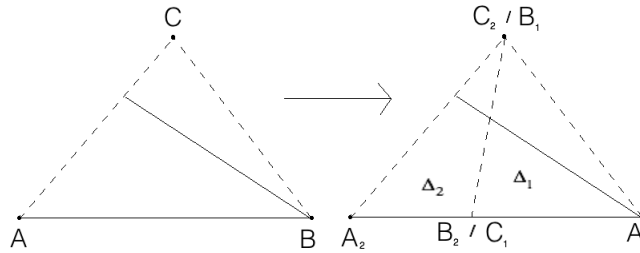


Figure 15: Making  $B$  into  $A$

Thus, we can assume that the edge has the vertex  $A$ . Now, if the edge crosses under  $BC$ , we can, through a series of Reidemeister moves, obtain a diagram of the Reidemeister move of type I as seen in Figure 16.

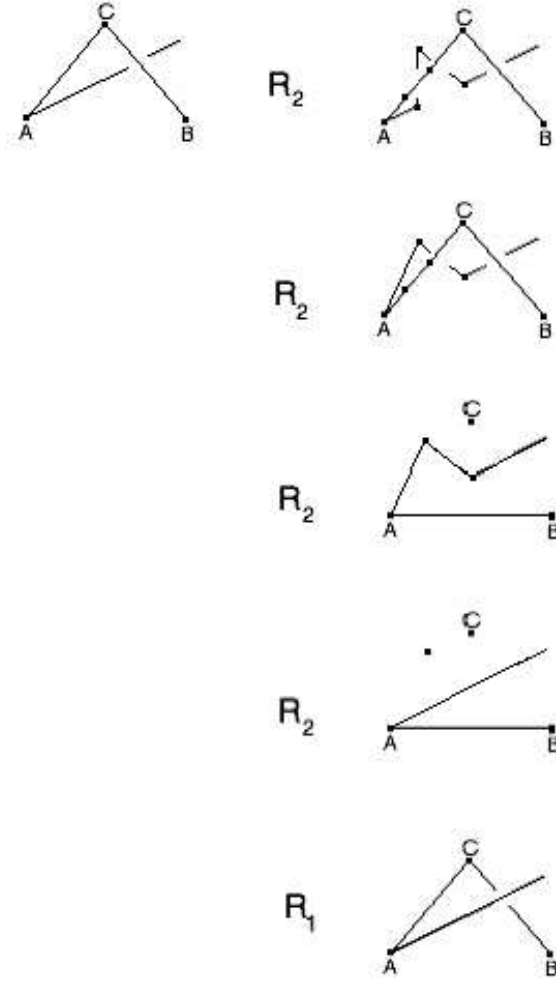


Figure 16: Obtaining the Reidemeister move of type I from a sequence of Reidemeister moves

Now, if the edge does not have a vertex in  $\Delta$ , then it crosses over/under two edges of  $\Delta$ . If one of the edges it crosses is  $AB$ , then it forms a triangular region in  $\Delta$  with either  $A$  or  $B$  as one of its vertexes. We construct a factorization  $(\Delta_i)_{i=1}^2$  where the edge does not cross through the ‘ $AB$ ’ edge in either of the factors, as seen in Figure 17.

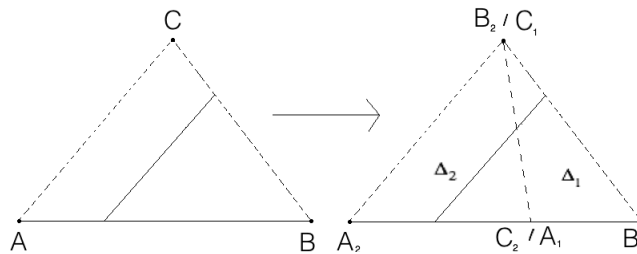


Figure 17: Making it so the edge does not cross through  $AB$



Then, all that is left is the case where the edge does not pass through a vertex nor the side  $AB$ . Note that if the edge crosses under (over) one of  $AC$  or  $BC$ , it must cross under (over) the other as well,  $\Delta$  is a valid  $\Delta$ -move. Now, if the edge crosses under  $AC$  and  $BC$ , then from a series of Reidemeister moves we can transform so that it crosses over instead, as seen in Figure 18. Note that if this is the case, then it is a diagram of the Reidemeister move of type II.  $\square$

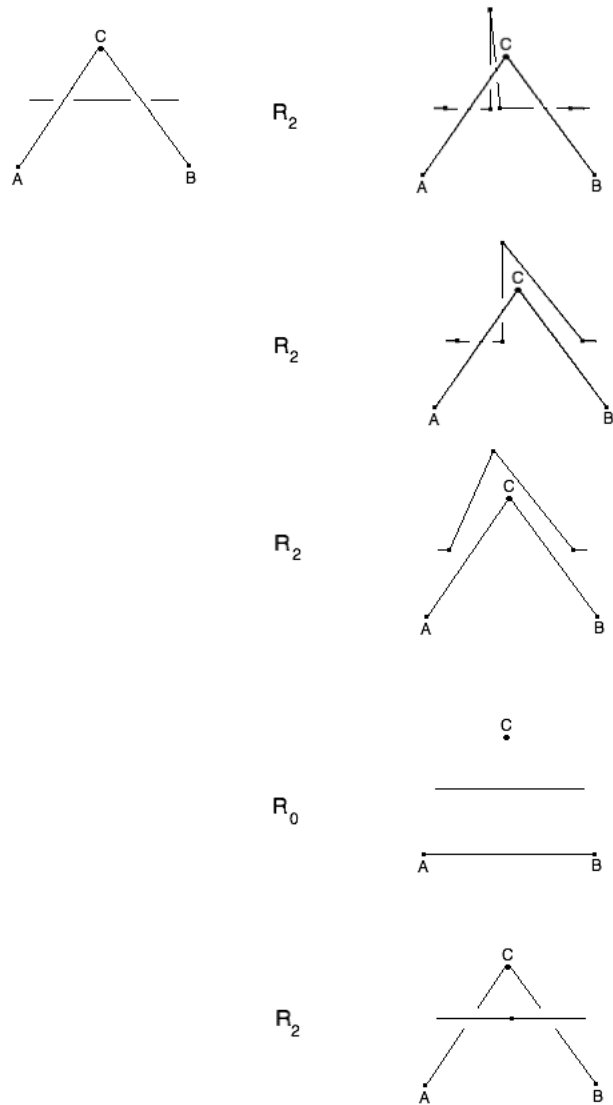


Figure 18: Obtaining the Reidemeister move of type II from a sequence of Reidemeister moves

The power of this theorem is that it allows us to check the invariance of mappings on links. Indeed, let  $\mathbf{D}$  denote the class of link diagrams, then a function  $V : \mathbf{D} \rightarrow \mathbf{X}$ , is a link invariant if and only if it is invariant under Reidemeister moves. That is, if  $V(D) = V(RD)$

for any link diagram  $D$ , where  $R$  is a Reidemeister move on  $D$  of type I, II, or III. Since there are only three cases to verify invariance, this is a very simple process.

**Definition 3.9.** The component of a link  $C : \mathbf{D} \rightarrow \mathbb{N}$ ,  $C(L)$  is given by the number of components in a link  $L$ .

Given a link diagram of  $L$ , it is easily shown that links varying by a Reidemeister move have the same number of components. Thus,  $C(L)$  is a link invariant that can be used to distinguish links having a different number of components. However, this does not demonstrate that the two-component unlink is different from the Hopf-link, nor that the trefoil is different than the unknot. In the next section, we develop more powerful link invariants that we can use to demonstrate these statements.

## 4 Link invariants

Up to this point, we have not been able to demonstrate that a knot are distinct from another, in particular, we have not shown that there are any knots other than the unknot. While the Reidemeister moves on knot diagrams provide a simple way of determining the equivalence of two knots, this does not help in the task of showing that two knots are distinct in a computationally efficient way: not being able to find a sequence of Reidemeister moves that relates two knots is *not* the same as demonstrating that there cannot be such a sequence. In this section, we will examine two simple link-invariants, the ‘linking number’ and the ‘Alexander–Conway polynomial’, which allow us to distinguish a number of links that we suspect are distinct.

### 4.1 Linking Number

Recall the orientation of a link, as discussed in Section 2.3. Consider an oriented link  $L$ . We can assign a ‘sign’ to each of the links crossings, based on the orientation of the strands in the crossing. The signs and their respective orientations are in Figure 19.



Figure 19: The sign of a crossing

Using these definitions, we define a function on the points of a link diagram:

$$\epsilon(p) = \begin{cases} 1 & \text{if } p \text{ is a positive crossing} \\ 0 & \text{if } p \text{ is not a crossing} \\ -1 & \text{if } p \text{ is a negative crossing} \end{cases}$$

With this notation, we can construct a new link invariant, the linking number.

**Definition 4.1.** (Generalized from Chapter II of [5]) The ‘linking number’ is a function  $\ell k : \mathbf{D} \rightarrow \mathbb{Z}$  defined by

$$\ell k(L) = \frac{1}{2} \sum_{\alpha, \beta \subset L} \sum_{p \in \alpha \cap \beta} \epsilon(p)$$

where  $\alpha$  and  $\beta$  are distinct components of  $L$ .

**Proposition 4.2.** The linking number is a link invariant.

*Proof.* To prove this, we only need to consider two links that are related by a single Reidemeister move. Furthermore, since the linking number is determined by the local structure of a link, we only need to consider the local changes made by the Reidemeister move.

In the case of the type I Reidemeister move, note that it is always the case that the crossing is formed by a single strand, thus the crossing point is not a crossing point between two distinct components, and it has no affect on the linking number.

In the case of the type II Reidemeister move, if the two strands belong to the same component, then the linking number is equivalent in the two diagrams by the same argument as above. Otherwise, note that regardless of the orientations of the strands, the local linking number in the diagram with crossings always sums to 0, since the two crossings are necessarily of opposite sign.

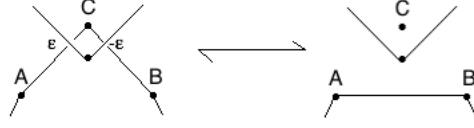


Figure 20: Invariance of  $R_2$

In the case of the type III Reidemeister move, note that all the crossing points remain the same with respect to their strands and crossing type, the only difference is their positions in the diagram. Indeed, then top left crossing becomes the bottom right, the top right becomes the bottom left, and the center remains the center.

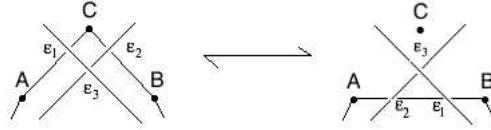


Figure 21: Invariance of  $R_3$

So, the linking number is invariant under Reidemeister moves, and thus it is a link invariant.  $\square$

Now, given the link invariant we have constructed, we can show that the Hopf link is distinct from the two component unlink. Indeed, as seen in Figure 22, the linking number of the 2-unlink is 0, while the linking number for the Hopf link is  $\pm 1$  dependent on orientation.

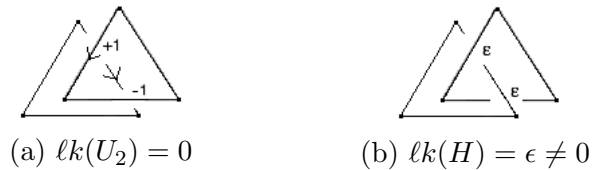


Figure 22: The linking numbers of the 2-unlink and a Hopf link

However, as one might realize, the linking number is not sufficient to classify all links. Indeed, the linking number of any two unlinks is 0, yet recalling  $C(L)$  from Definition 3.9.,  $C(U_n) = n$  for the  $n$ -unlink, then  $U$  and  $U_2$  are distinct, since  $C(U) \neq C(U_2)$ .

Here is a less trivial example. A link  $B$  is said to be Brunnian, if it is a non-trivial link with the property that deleting any of its components results in an unlink.

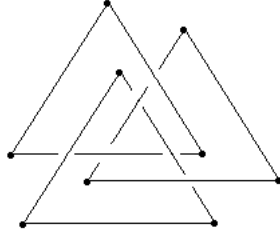


Figure 23: A Brunnian link

From this property, we can see that if  $B$  has three or more components, then each pairing of components must be unlinked with respect to one another. Thus, the linking number of a Brunnian link of three or more components is 0. Given our current set of tools we cannot actually determine if any such links exist, since we cannot distinguish a potentially Brunnian link from an unlink.

## 4.2 The Alexander–Conway Polynomial

In 1923 James Alexander defined what is likely the first important link invariant, the Alexander Polynomial. However, given a link  $K$ , computing its Alexander Polynomial can be a lengthy and computationally difficult task. In 1963, John Conway redefined the Alexander Polynomial using only three axioms, and the introduction of an important concept in combinatoric knot theory, the skein relation.

**Definition 4.3.** A skein relation is a triple of link diagrams that differ only in a single neighbourhood of the plane, as shown in Figure 24.

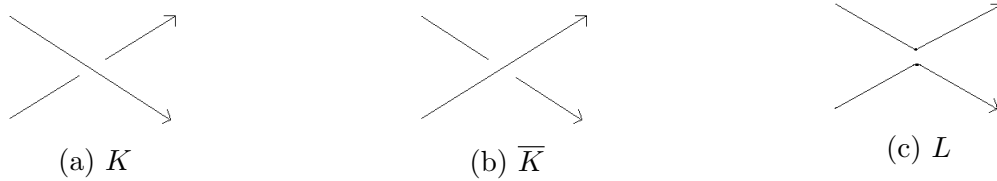


Figure 24: The skein relation

An example of three knots in a skein relationship can be found in Figure 25.

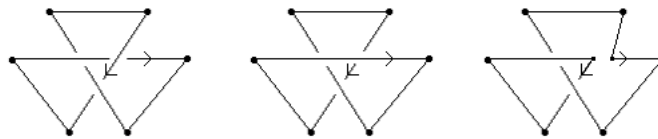


Figure 25: The trefoil, unknot, and Hopf link are skein related

In this example, we see that many characteristics of a knot can change significantly by modifying only a small part of it. Indeed, we see in the figure that a trefoil is skein related to an unknot and a Hopf link.

With an understanding of the skein relation, we can proceed to define the Alexander–Conway Polynomial. Recall that if  $R$  is a ring, then  $R[x]$  denotes the ring of polynomials with coefficients in  $R$ .

**Definition 4.4.** (p. 19 of [5]) The Alexander–Conway Polynomial of a link  $K$ ,  $\nabla_K(z) \in \mathbb{Z}[z]$ , is defined by the following three axioms:

- (i) If  $K$  and  $K'$  are equivalent as oriented links, then  $\nabla_K(z) = \nabla_{K'}(z)$ .
- (ii) If  $U$  is the unknot, then  $\nabla_U(z) = 1$ .
- (iii) If  $K$ ,  $\overline{K}$ , and  $L$  are oriented links related by the standard skein relation, then  $\nabla_K(z) - \nabla_{\overline{K}}(z) = z\nabla_L(z)$ .

Even though we do not give a proof, these axioms are consistent, and thus the Alexander–Conway polynomial defines a link invariant. However, the axioms do not provide a simple way to compute the Alexander–Conway polynomial of a link. So before we attempt to compute directly the Alexander–Conway polynomials of any link, we will prove a few properties of the polynomial itself.

**Definition 4.5.** A link  $L$  is called split if it is equivalent to a link with a diagram such that there are  $A, B \subset \mathbb{R}^2$  with  $A \cap B = \emptyset$ ,  $L \subset A \cup B$ ,  $A \cap L \neq \emptyset$  and  $B \cap L \neq \emptyset$

Less formally, a link is split if it comes in two or more separate components. This idea is captured in Figure 26.

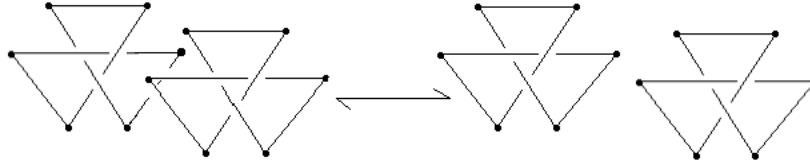


Figure 26: An example of a split link

It turns out that the Alexander–Conway polynomial of a split link is very simple.

**Proposition 4.6.** (p. 20 of [5]) If  $L$  is an oriented split link, then  $\nabla_L(z) = 0$

*Proof.* Given that  $L$  has two separate components, we may form two new links  $K$  and  $\overline{K}$ , such that  $K$ ,  $\overline{K}$  and  $L$  form the usual skein relationship (refer to Figure 27 below).  $K$  and  $\overline{K}$  are equivalent (twist  $K_2$  by  $2\pi$  clockwise along the vertical axis in  $\overline{K}$  via  $\Delta$ -moves in  $\mathbb{R}^3$ ) so  $\nabla_K(z) = \nabla_{\overline{K}}(z)$  by axiom (i). Then, by axiom (iii),  $z\nabla_L(z) = 0$ , so  $\nabla_L = 0$ .  $\square$

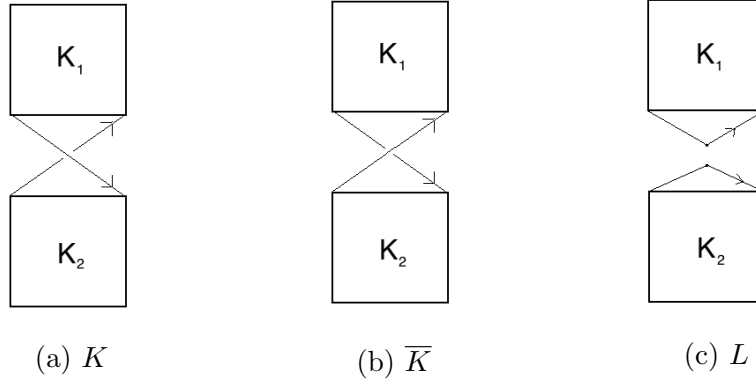


Figure 27: A split link skein relation

From this proposition, it follows that if  $U_n$  is an  $n$ -component unlink, with  $n \geq 2$ , that  $\nabla_{U_n}(z) = 0$ .

With this additional fact, we can now easily compute the Alexander–Conway polynomial of the trefoil, as seen in Figure 28.

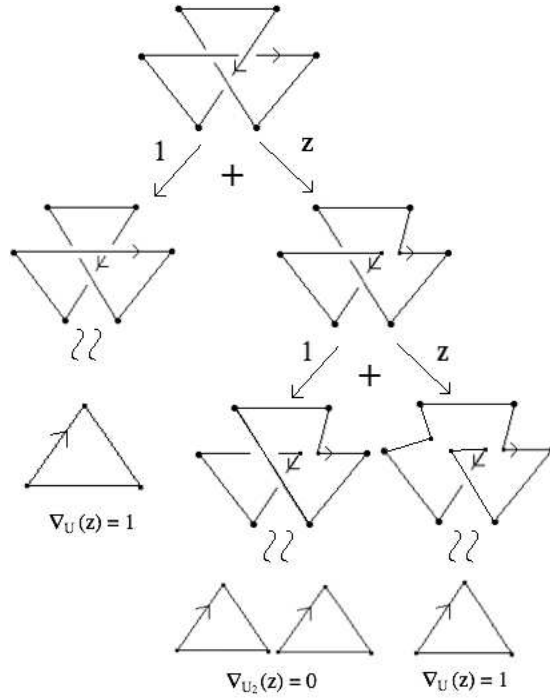


Figure 28: The Alexander–Conway polynomial of a trefoil is  $1 + z^2$

Since the Alexander–Conway polynomial of the trefoil is different from the one of the unknot, we have shown that there is indeed a non-trivial knot.

Although the Alexander–Conway polynomial does allow us to distinguish many knots, it has its drawbacks. One of which is its inability to determine if a knot is chiral, that is, non-equivalent to its mirror image.

**Definition 4.7.** Let  $K$  be a link. Then its mirror image  $K^!$  is the knot whose diagram is obtained from the diagram of  $K$  by switching all of its crossings.

**Proposition 4.8.** Let  $K$  be an oriented link. Then  $\nabla_{K^!}(z) = (-1)^{C(K)+1} \nabla_K(z)$ .

*Proof.* We proceed by induction on the number of crossings points in the diagram of  $K$ .

If  $K$  has 0 crossing points, then  $K$  is either the unknot or an unlink. In each case,  $K^! = K$ . Thus their polynomials are equal. In the case of an unknot, the factor  $(-1)^{C(K)+1}$  is just 1, so the proposition holds. In the other cases, both polynomials are zero since both  $K$  and  $K^!$  are split.

Now, suppose the statement holds for any link with  $n$  crossings. Consider a link with  $n + 1$  crossings.

We compute  $\nabla_K - \nabla_{K^!}$ . By Axiom (iii), if we switch a crossing in  $K$  with sign  $\epsilon$  then,

$$\nabla_K = \nabla_{\overline{K}} + z\epsilon \nabla_L$$

where  $\overline{K}$  is obtained by switching the crossing, and  $L$  is obtained by splitting the crossing. Similarly, we can see that

$$\nabla_{K^!} = \nabla_{\overline{K}^!} - z\epsilon \nabla_{L^!}$$

Now,  $L$  and  $L^!$  have  $n$  crossings, so by the induction hypothesis

$\nabla_{L^!} = (-1)^{C(L)+1} \nabla_L$ , thus

$$\nabla_K - \nabla_{K^!} = (\nabla_{\overline{K}} - \nabla_{\overline{K}^!}) + z\epsilon(\nabla_L + (-1)^{C(L)+1} \nabla_L)$$

We can proceed in this same way with the  $\nabla_{\overline{K}} - \nabla_{\overline{K}^!}$  term until  $\overline{K}$  is an unlink (we take it as an unproven fact that there is a switching crossings for any link that gives the unlink). Clearly  $\overline{K}^!$  is also an unlink, so  $\nabla_{\overline{K}} - \nabla_{\overline{K}^!} = 0$ . Thus,  $\nabla_K - \nabla_{K^!}$  is just a sum of terms of the form  $z\epsilon(\nabla_L + (-1)^{C(L)+1} \nabla_L)$ .

If  $C(K)$  is odd, then  $C(L)$  is even, so all terms in the sum are 0, and thus  $\nabla_K = \nabla_{K^!}$ .

If  $C(K)$  is even, then  $C(L)$  is odd, so all terms in the sum are of the form  $2z\epsilon \nabla_L$ , and moreover the sum of these terms is twice  $\nabla_K$ , since  $\nabla_K = \nabla_{\overline{K}} + \sum z\epsilon \nabla_L$ , and  $\nabla_{\overline{K}} = 0$  (since  $\overline{K}$  is an unlink with even component). Thus,  $\nabla_K = -\nabla_{K^!}$ .  $\square$

Thus, the Alexander–Conway polynomial is incapable of distinguishing chiral knots, or more generally chiral links with odd component, since  $\nabla_K = \nabla_{K^!}$  for these. However, if  $K$  has even component and  $\nabla_K \neq 0$  then  $K$  is chiral.



## 5 The Jones Polynomial

At the end of the last section, we found that the Alexander–Conway polynomial is incapable of distinguishing chiral links with odd component. The linking number is no help in this regard either, since it does not provide any information at all about a knot.

In this section, we introduce the Jones Polynomial, a link invariant found by Vaughan Jones in 1984. Later on, Louis Kauffman expanded further Jones’ study of knot polynomials, allowing for a much simpler presentation of the Jones polynomial.

### 5.1 The Kauffman Bracket

We start by discussing the notion of a link state. Consider an arbitrary crossing in a link diagram. If the diagram is unoriented, then we can define a splitting procedure on this crossing, in a way that is reminiscent of the skein relations in Section 4.2. Here we have fewer restrictions: we no longer need to worry about maintaining a consistent orientation for the link. This allows each crossing to be split in two different ways, as shown below.

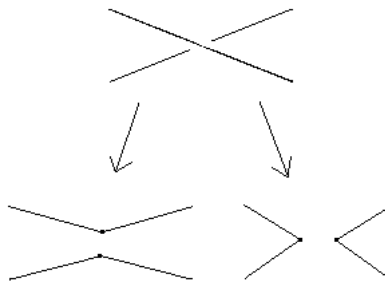
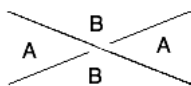
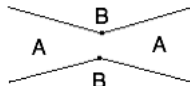


Figure 29: Two ways of splitting a crossing

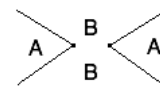
Moreover, we may distinguish exactly what type of split we have made through the following convention. Align the diagram so that the crossing appears like in Figure 30 (a), and label the regions formed by the crossing with A’s and B’s, as in the diagram. A helpful way remember the labelling is to imagine a person is standing atop the upper strand, facing the crossing: the region A will be to their right, and the region B to their left. Then, an A-split is the split that joins the A regions together, while a B split joins the B regions together.



(a) Marking



(b) A-Split



(c) B-Split

Figure 30: Labelling Splits

Given the link diagram of  $K$ , we define a state  $\sigma$  of  $K$  as the diagram obtained by splitting all of the crossings of  $K$  by some combination of A and B-splits. Then a link diagram with  $n$  crossings in its diagram has  $2^n$  states, and the set of all these states is

denoted by  $S(K)$ . Given a state  $\sigma$  of a link diagram  $K$  that uses  $n$  A-splits and  $m$  B-splits, define  $\langle K|\sigma \rangle = A^n B^m$ , and  $\|\sigma\| = C(\sigma) - 1$ . We can now define the Kauffman bracket.

**Definition 5.1.** (Definition 3.1 of [4]) Let  $A$ ,  $B$  and  $d$  be commutative variables. The Kauffman bracket is a mapping  $\langle \rangle : \mathbf{D} \rightarrow \mathbb{R}[A, B, d]$  defined by

$$\langle K \rangle = \sum_{\sigma \in S(K)} \langle K|\sigma \rangle d^{\|\sigma\|}$$

This definition however is computationally cumbersome. Potentially, one would be required to identify every state of a link diagram  $K$ , and  $|S(K)|$  increases exponentially with respect to the number of crossings in  $K$ . Therefore, we would like to identify some features of the Kauffman bracket that will allow for simple computations.

**Proposition 5.2.** (See [3]) If the links diagrams  $K$ ,  $K_A$ , and  $K_B$  are related as in Figure 30, then

$$\langle K \rangle = A\langle K_A \rangle + B\langle K_B \rangle$$

Also, if a link is a union of a knot  $U$  without crossings, and another link  $K$ , such that  $U$  and  $K$  are split, then

$$\langle K \cup U \rangle = d \cdot \langle K \rangle$$

*Proof.* For the first part of the proposition, note that  $S(K_A) \cup S(K_B) = S(K)$  and  $S(K_A) \cap S(K_B) = \emptyset$ . Also, if  $\sigma$  is a state of both  $K$  and  $K_A$ , then  $\langle K|\sigma \rangle = A\langle K_A|\sigma \rangle$ , since the crossing in the skein relation is only an A-split for  $K$ . Similarly,  $\langle K|\sigma \rangle = B\langle K_B|\sigma \rangle$ . Thus, we can see that

$$\begin{aligned} \langle K \rangle &= \sum_{\sigma \in S(K)} \langle K|\sigma \rangle d^{\|\sigma\|} \\ &= \sum_{\lambda \in S(K_A)} A\langle K_A|\lambda \rangle d^{\|\lambda\|} + \sum_{\theta \in S(K_B)} B\langle K_B|\theta \rangle d^{\|\theta\|} \\ &= A\langle K_A \rangle + B\langle K_B \rangle \end{aligned}$$

For the second half of the proposition, note that each state of  $K \cup U$  is  $\sigma \cup U$ , where  $\sigma$  is a state of  $K$ . Also, since  $U$  has no crossings,  $\langle K \cup U|\sigma \cup U \rangle = \langle K|\sigma \rangle$ , and  $\|\sigma \cup U\| = \|\sigma\| + 1$ . Then, we see that

$$\begin{aligned} \langle K \cup U \rangle &= \sum_{\sigma \in S(K)} \langle K \cup U|\sigma \cup U \rangle d^{\|\sigma \cup U\|} \\ &= \sum_{\sigma \in S(K)} \langle K|\sigma \rangle d^{\|\sigma\|+1} \\ &= d\langle K \rangle \end{aligned}$$

□

This computational shortcut will allow us to check if the Kauffman bracket is a link invariant quite easily.

**Proposition 5.3.** (Corollary 3.4 and Proposition 3.5 of [4]) If  $B = A^{-1}$ , and  $d = -A^2 - A^{-2}$ , then the Kauffman bracket is invariant under the Reidemeister moves of type II and III, but not type I.

*Proof.* This proof is entirely diagrammatic. Rather than drawing the entirety of the link diagram inside the Kauffman brackets, we instead only draw the neighbourhood we are interested in.

First we show that the bracket is invariant under the Reidemeister move of type II.

$$\begin{aligned}
\langle \text{Diagram 1} \rangle &= A \langle \text{Diagram 2} \rangle + A^{-1} \langle \text{Diagram 3} \rangle \\
&= A^2 \langle \text{Diagram 4} \rangle + \langle \text{Diagram 5} \rangle + \langle \text{Diagram 6} \rangle + A^{-2} \langle \text{Diagram 7} \rangle \\
&= \langle \text{Diagram 8} \rangle + ((A^2 + A^{-2}) + (-A^2 - A^{-2})) \langle \text{Diagram 9} \rangle \\
&= \langle \text{Diagram 8} \rangle
\end{aligned}$$

Next we show the bracket is invariant under the Reidemeister move of type III. Note that throughout we use the invariance of the bracket under the Reidemeister move of type II.

$$\begin{aligned}
\langle \text{Diagram 1} \rangle &= A \langle \text{Diagram 2} \rangle + A^{-1} \langle \text{Diagram 3} \rangle \\
&= A \langle \text{Diagram 4} \rangle + A^{-1} \langle \text{Diagram 5} \rangle \\
&= A \langle \text{Diagram 6} \rangle + A^{-1} \langle \text{Diagram 7} \rangle
\end{aligned}$$

$$\begin{aligned}
&= A \left\langle \begin{array}{c} \diagup \quad \diagdown \\ \hline \triangle \\ \hline \diagdown \quad \diagup \end{array} \right\rangle + A^{-1} \left\langle \begin{array}{c} \diagup \quad \diagdown \\ \hline \triangle \\ \hline \diagup \quad \diagdown \end{array} \right\rangle \\
&= \left\langle \begin{array}{c} \diagup \quad \diagdown \\ \hline \diagdown \quad \diagup \end{array} \right\rangle
\end{aligned}$$

Last, we show that the bracket is not invariant under Reidemeister moves of type I.

$$\begin{aligned}
\left\langle \begin{array}{c} \diagup \\ \diagdown \end{array} \right\rangle &= A \left\langle \begin{array}{c} \diagup \\ \diagdown \end{array} \right\rangle + A^{-1} \left\langle \begin{array}{c} \diagdown \\ \diagup \end{array} \right\rangle \\
&= (-A^3 - A^{-1}) \left\langle \begin{array}{c} \diagup \\ \diagdown \end{array} \right\rangle + A^{-1} \left\langle \begin{array}{c} \diagup \\ \diagdown \end{array} \right\rangle \\
&= -A^3 \left\langle \begin{array}{c} \longrightarrow \end{array} \right\rangle
\end{aligned}$$

Using this computation, we see that the Kauffman bracket is not invariant for the unknot.

$$\begin{aligned}
\left\langle \begin{array}{c} \diagup \\ \diagdown \end{array} \right\rangle &= -A^3 \\
\left\langle \begin{array}{c} \triangle \end{array} \right\rangle &= 1
\end{aligned}$$

□

Henceforth, when we refer to the Kauffman bracket, we are referring to the case in which the variables are as in Proposition 5.3. In the last section of the proof, we saw that  $\langle K \rangle = -A^{-3} \langle R_1 K \rangle$  (where  $R_1 K$  is a Reidemeister move of type  $R_1$  applied to  $K$ ). This gives us some intuition as to how we might normalize the Kauffman bracket. To do so, we introduce the notion of *writhe*.

## 5.2 The Normalized Kauffman Bracket

**Definition 5.4.** (Definition 3.6 of [4]) The *writhe* of an oriented link  $K$ , denoted  $w(K)$ , is the sum of its crossing signs,  $w(K) = \sum_{p \in Cr(K)} \epsilon(p)$ , where  $Cr(K)$  is the set of  $K$ 's crossing points.

Clearly  $w(K)$  is not itself a link invariant, as two oriented knot diagrams related by Reidemeister move of type I have different writhes. However, it is easily shown that like the Kauffman bracket, it is invariant under Reidemeister moves of types II and III. So, we want to define a link mapping  $f$  that is determined by the writhe of a knot, satisfying  $f(w(K)) = -A^3 f(w(R_1 K))$ . We define such a function as  $(-A^3)^{-w(K)}$ .

**Definition 5.5.** The Normalized Kauffman Bracket of an oriented link  $K$ ,  $\mathcal{L} : \mathbf{D} \rightarrow \mathbb{R}[A]$  is defined by  $\mathcal{L}_K = (-A^3)^{-w(K)} \langle K \rangle$ .

**Proposition 5.6.** (Proposition 3.7 of [4])  $\mathcal{L}$  is a link invariant.

*Proof.* Both terms in the definition are invariant under Reidemeister moves of type II and III, and so their product  $\mathcal{L}$  is invariant under these moves as well.

Performing a Reidemeister move of type I to  $K$ , we know that  $\langle K \rangle = (-A^{-3}) \langle R_1 K \rangle$  from the proof of Proposition 5.3., and  $w(K) = w(R_1 K) + 1$ , so  $(-A^3)^{-w(K)} = (-A^3)^{-w(R_1 K)-1}$ . Thus,

$$\begin{aligned} \mathcal{L}_K &= (-A^3)^{-w(K)} \langle K \rangle \\ &= (-A^3)^{-w(R_1 K)-1} (-A^3) \langle R_1 K \rangle \\ &= (-A^3)^{-w(R_1 K)} \langle R_1 K \rangle \\ &= \mathcal{L}_{R_1 K} \end{aligned} \quad \square$$

We now have another tool to aid in the classification of links. One major advantage of the normalized Kauffman bracket as compared to the Alexander–Conway polynomial is its potential to identify chiral knots.

**Proposition 5.7.** If  $K$  is a link, then  $\mathcal{L}_{K^!}(A) = \mathcal{L}_K(A^{-1})$ .

*Proof.* To begin, note a few facts. First,  $w(K^!) = -w(K)$ , since the signs of all  $K^!$ 's crossings are opposite in  $K$ . Second, if  $\sigma$  is a state of  $K^!$ , then it is also a state of  $K$ , and vice versa. However,  $\langle K^! | \sigma \rangle = \langle K | \sigma \rangle^{-1}$ , since the same state is obtained by taking the opposite splits at each crossing, which means that the  $A$ -splits of  $K$  are the  $A^{-1}$ -splits of  $K^!$ . Lastly,  $-A^2 - A^{-2} = -(A^{-1})^2 - (A^{-1})^{-2}$ . So,

$$\begin{aligned} \mathcal{L}_{K^!}(A) &= (-A^3)^{-w(K^!)} \langle K^! \rangle \\ &= (-A^3)^{w(K)} \sum_{\sigma \in S(K^!)} \langle K^! | \sigma \rangle (-A^2 - A^{-2})^{\|\sigma\|} \\ &= (-(A^{-1})^3)^{-w(K)} \sum_{\sigma \in S(K)} \langle K | \sigma \rangle^{-1} (-(A^{-1})^2 - (A^{-1})^{-2})^{\|\sigma\|} \\ &= \mathcal{L}_K(A^{-1}) \end{aligned} \quad \square$$

Immediately, we can see that if the normalized Kauffman bracket of a knot  $K$  is not a symmetric Laurent polynomial ( $a_n = a_{-n}$  for all  $n$ ), then  $K$  is a chiral knot!

### 5.3 The Jones Polynomial

**Definition 5.8.** The Jones Polynomial of an oriented link  $K$ , denoted by  $V_K$ , is a Laurent polynomial in the variable  $\sqrt{t}$  defined by the axioms

- (i) If  $K$  and  $K'$  are equivalent as oriented links, then  $V_K(t) = V_{K'}(t)$ .
- (ii) If  $U$  is the unknot, then  $V_U(t) = 1$ .
- (iii) If  $K$ ,  $\overline{K}$ , and  $L$  are oriented links related by the standard skein relation, then we have the following equality:

$$t^{-1}V_K(t) - tV_{\overline{K}}(t) = (\sqrt{t} - \frac{1}{\sqrt{t}})V_L(t)$$

**Theorem 5.9.** (Theorem 5.2. of [4])  $\mathcal{L}_K(t^{-1/4}) = V_K(t)$ .

*Proof.* To verify the theorem, it is enough to check that  $\mathcal{L}_K(t^{-1/4})$  satisfies the three defining axioms of the Jones polynomial. Proposition 5.6. shows that  $\mathcal{L}_K(t^{-1/4})$  satisfies the first axiom. Obviously the normalized Kauffman Bracket of the unknot is 1, and changing variables from  $A$  to  $t^{-1/4}$  does not change this, so  $\mathcal{L}_K(t^{-1/4})$  satisfies the second axiom as well. To show that  $\mathcal{L}_K(t^{-1/4})$  satisfies the third axiom, we resolve to diagrammatic equations.

$$\begin{array}{c} \text{Diagram 1} \\ \text{Diagram 2} \end{array} = A \begin{array}{c} \text{Diagram 3} \\ \text{Diagram 4} \end{array} + A^{-1} \begin{array}{c} \text{Diagram 5} \\ \text{Diagram 6} \end{array} \quad (1)$$

$$\begin{array}{c} \text{Diagram 7} \\ \text{Diagram 8} \end{array} = A^{-1} \begin{array}{c} \text{Diagram 9} \\ \text{Diagram 10} \end{array} + A \begin{array}{c} \text{Diagram 11} \\ \text{Diagram 12} \end{array} \quad (2)$$

Multiplying equation (1) by  $A$ , and equation (2) by  $A^{-1}$ , and subtracting them, we obtain

$$A \begin{array}{c} \text{Diagram 1} \\ \text{Diagram 2} \end{array} - A^{-1} \begin{array}{c} \text{Diagram 7} \\ \text{Diagram 8} \end{array} = (A^2 - A^{-2}) \begin{array}{c} \text{Diagram 3} \\ \text{Diagram 4} \end{array} \quad (3)$$

Consider the writhe,  $w$  of the link in the bracket on the right hand side of the equation. Then the other two knots have writhes  $w + 1$  and  $w - 1$  respectively.

Thus, by multiplying equation (3) by  $(A^3)^{-w}$ , we obtain

$$-A^4(-A^3)^{-(w+1)} \begin{array}{c} \text{Diagram 1} \\ \text{Diagram 2} \end{array} + A^4(-A^3)^{-(w-1)} \begin{array}{c} \text{Diagram 7} \\ \text{Diagram 8} \end{array} = (A^2 - A^{-2})(-A^3)^{-w} \begin{array}{c} \text{Diagram 3} \\ \text{Diagram 4} \end{array}$$

Which is just,

$$-A^4 \mathcal{L}_K(A) + A^{-4} \mathcal{L}_{\overline{K}}(A) = (A^2 - A^{-2}) \mathcal{L}_L(A).$$

Setting  $A = t^{-1/4}$  and multiplying through by  $-1$ , we see the third axiom holds as well

$$t^{-1}\mathcal{L}_K(t^{-1/4}) - t\mathcal{L}_{\overline{K}}(t^{-1/4}) = (\sqrt{t} - \frac{1}{\sqrt{t}})\mathcal{L}_L(t^{-1/4}). \quad \square$$

We conclude this section by computing the Jones polynomial of the Hopf link, the right-handed trefoil, and its mirror image.

For the Hopf link  $H$ , we choose its orientation to be so that it is as in Figure 22. Then  $w(H) = 2$ . We compute the Kauffman bracket of  $H$ .

$$\begin{aligned}
\langle \text{Hopf link } H \rangle &= A \langle \text{Hopf link } H \rangle + A^{-1} \langle \text{Hopf link } H \rangle \\
&= A^2 \langle \text{Hopf link } H \rangle + \langle \text{Hopf link } H \rangle + \langle \text{Hopf link } H \rangle + A^2 \langle \text{Hopf link } H \rangle \\
&= A^2(-A^2 - A^{-2}) + 1 + 1 + A^{-2}(-A^2 - A^{-2}) \\
&= -A^4 - 1 + 1 + 1 - 1 - A^{-4} \\
&= -A^4 - A^{-4}
\end{aligned}$$

So,  $V_H(t) = (-t^{-3/4})^{-2}(-t^{-1} - t) = t^{5/2} + t^{1/2}$ .

For the right-handed trefoil  $T$ , note that its writhe is the same regardless of orientation, and  $w(T) = 3$ . We compute the Kauffman bracket of  $T$ , using our computation of  $\langle H \rangle$  in the second line.

$$\begin{aligned}
\langle \text{Trefoil } T \rangle &= A \langle \text{Trefoil } T \rangle + A^{-1} \langle \text{Trefoil } T \rangle \\
&= -A^5 - A^{-3} + \langle \text{Trefoil } T \rangle + A^{-2} \langle \text{Trefoil } T \rangle \\
&= -A^5 - A^{-3} + (1 + A^{-2})(-A^2 - A^{-2}) \langle \text{Trefoil } T \rangle
\end{aligned}$$

$$\begin{aligned}
&= -A^5 - A^{-3} - A^{-4} \left\langle \text{Diagram 1} \right\rangle \\
&= -A^5 - A^{-3} - A^{-3} \left\langle \text{Diagram 2} \right\rangle - A^{-5} \left\langle \text{Diagram 3} \right\rangle \\
&= -A^5 - A^{-3} - A^{-3} - A^{-5}(-A^2 - A^{-2}) \\
&= -A^5 - A^{-3} + A^{-7}
\end{aligned}$$

So,  $V_T(t) = (-t^{-3/4})^{-3}(-t^{-5/4} - t^{3/4} + t^{7/4}) = -t^4 + t^3 + t$ . Using this and proposition 5.7, the left-handed trefoil  $\overline{T}$ , has  $V_{\overline{T}}(t) = -t^{-4} + t^{-3} - t^{-1}$ , showing the trefoil is chiral.



## 6 Applications to Molecular Biology

While our discussion has predominantly focussed on purely mathematical ideas, knot theory is a useful tool for studying natural phenomena. In this section, we will briefly examine how knot theory was used by molecular biologists to study DNA, following the discussion found in Chapter 13 of [6].

### 6.1 Supercoiling

Assuming the reader has some familiarity with molecular biology, we know that (human) DNA is not by our definition a knot. However, in laboratory settings DNA may be seen to form a closed ring structure, so our knot theoretic analysis may be used. Also, since our theory is based on the diagrams of knots, it lends itself well to molecular biology, as the images of ringed DNA resemble link diagrams greatly. Note also that while DNA may be ‘smooth’ to some degree, we will continue with our convention of knots being polygonal.

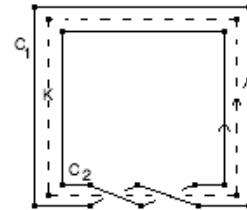
Although the topology of the DNA molecule is unrelated to its chemical structure, contemporary research has indicated that its topology does correspond to its function in the cell. Since DNA is often double-stranded, its ringed form may be assigned a linking number as in section 4.1, where the components of the link are simply the closed forms of the strands.

Moreover, as shown in Figure 31, the strands  $C_1$  and  $C_2$  of DNA are also part of the boundary of an embedding of  $\mathbb{S}^1 \times [-1, 1]$ , which is commonly referred to as a ribbon. Let  $R$  denote the image of the embedding. On the surface of  $R$  itself, we may embed a knot  $K$  given by the image of  $\mathbb{S}^1 \times \{0\}$ , which serves as an axis of reference. Choosing an orientation for  $K$ , we may also assign  $C_1$  and  $C_2$  orientations that agree with  $K$ . The two values we are concerned with assigning the ribbon are its writhe, and its twist. Here, the writhe of a ribbon  $w(R)$  can be thought of as  $w(K)$  Definition 5.4. The twist of a ribbon  $Tw(R)$  refers to the number of rotations  $C_1$  and  $C_2$  make about  $K$ . It is a property of ribbons that if  $L$  is the link formed by  $C_1$  and  $C_2$ , then

$$\ell k(L) = w(R) + Tw(R)$$



(a)  $\ell k(L) = -1$ ,  $w(R) = -1$ ,  $Tw(R) = 0$



(b)  $\ell k(L) = 1$ ,  $w(R) = 0$ ,  $Tw(R) = 1$

Figure 31: Diagrams of DNA

In the context of DNA, the twist of a DNA molecule relates roughly to the amount of tension due to the helical structure of the DNA. Since  $\ell k$  is an invariant, if a DNA molecule is put under greater helical tension, this is relieved by the writhing of the molecule in the other direction, a phenomena called *supercoiling*.

## 6.2 Recombination

In this section, because we are less concerned with the helical structure of DNA we adopt a new knot theoretic model of DNA. In this model, both strands are treated as though they are a unit, so that we obtain a model that can only demonstrate the supercoiling of the DNA strand - moreover this model will be a knot.

DNA recombination is a process by which segments of DNA are rearranged within the strand, so that the biological information encoded on the rearranged strand differs from the original. In the case of site-specific recombination, this rearrangement is brought about by an enzyme (*recombinase*) that draws together two points of the strand via supercoiling, and then causes the DNA molecule to be cut and recombined. A simple example of this process uses our knot theoretic model is given in Figure 32.

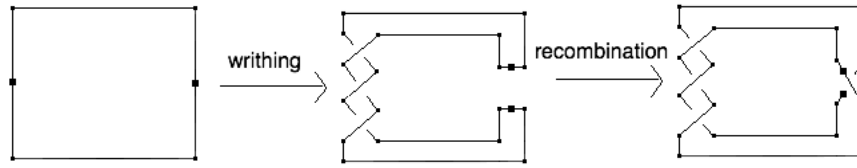


Figure 32: Site Specific Recombination

What we wish to determine is exactly what the above figure looks like in the case of specific enzymes. To refine what we mean by this, we make the supposition that all the knots obtained in the recombinant process can be expressed as the numerator of the sum of tangles (based on empirical observation). Briefly, a tangle is formed by taking 2 pairs of distinct points on  $\mathbb{S}^2$ , and connecting each of the pairs by a polygonal curve in  $\mathbb{B}^3$ , such that the curves do not intersect. Given two tangles, one may associate to them another tangle called the sum, and a knot called the numerator, illustrated in Figure 33.

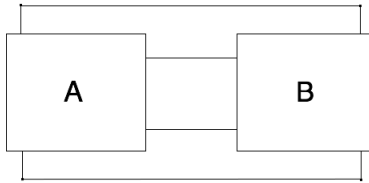


Figure 33: Numerator of the sum of tangles  $A$  and  $B$ ,  $N(A + B)$

We make the supposition that the knot given by writhing is  $N(S + E)$ , and the that the knot given by  $n$  site specific recombinations is given by  $N(S + R + \dots + R)$ , where  $R$  occurs  $n$  times in the sum, where  $S$  is the substrate,  $E$  is the enzyme, and  $R$  is recombination. From this, one obtains a system of equations that determine the tangles  $S$  and  $R$  uniquely, and restricts  $E$  a class of tangles. Knowing this provides the molecular biologist with a very strong understanding of the action of *recombinase*.

## References

- [1] J. Alexander and G. Briggs. On types of knotted curves, 1926-1927.
- [2] P. Cromwell. *Knots and links*. Cambridge University Press, 2004.
- [3] D. Evans. Lecture notes on knot theory, 2017.
- [4] L. H. Kauffman. *Knots and physics*. Series on Knots and Everything. World Scientific Publishing Company, 2nd edition, 1994.
- [5] L. H. Kauffman. *On knots*. Princeton University Press, 1987.
- [6] K. Murasugi. *Knot theory and its applications*. Birkhäuser, 1996.
- [7] J. H. Przytycki. Classical roots of knot theory, 1998.
- [8] J. Roberts. Knot knotes, March 1999.